This is a post-print (peer-reviewed) version of: Inglis., et al. (2018) Distributions of geohopanoids in peat: implications for the use of hopanoid-based proxies in natural archives, Geochimica et Cosmochimica Acta, 224, 249-261, doi: 10.1016/j.gca.2017.12.029. © 2018. This manuscript version is made available under the CC-BY-NC-ND 4.0 license

Distributions of geohopanoids in peat: implications for the use of hopanoid-based proxies in natural archives

Gordon N. Inglis[a,b*], B. David A. Naafs[a,b], Yanhong Zheng[c], Erin L. McClymont[d], Richard P. Evershed[a,b] and Richard D. Pancost[a,b] and the 'T-GRES Peat Database collaborators'

[a] Organic Geochemistry Unit, School of Chemistry, University of Bristol, Cantock's Close, Bristol, BS8 1TS, UK

[b] Cabot Institute, University of Bristol, Bristol, UK

[c] State Key Laboratory of Continental Dynamics, Department of Geology, Northwest University, Xi'an, PR China

[d] Department of Geography, Durham University, Durham, UK

Corresponding author: Gordon N. Inglis

Email: gordon.inglis@bristol.ac.uk. Telephone: +44 (0)117 954 6395

Abstract

Hopanoids are pentacyclic triterpenoids produced by a wide range of bacteria. Within modern settings, hopanoids mostly occur in the biological 17β,21β(H) configuration. However, in some modern peatlands, the C_{31} hopane is present as the 'thermally-mature' 17α,21β(H) stereoisomer. This has traditionally been ascribed to isomerisation at the C-17 position catalysed by the acidic environment. However, recent work has argued that temperature and/or hydrology also exert a control upon hopane isomerisation. Such findings complicate the application of geohopanoids as palaeoenvironmental proxies. However, due to the small number of peats that have been studied, as well as the lack of peatland diversity sampled, the environmental controls regulating geohopanoid isomerisation remain poorly constrained. Here, we undertake a global approach to investigate the occurrence, distribution and diagenesis of geohopanoids within peat, combining previously published and newly generated data (n = 395) from peatlands with a wide temperature (-1 to 27°C) and pH (3 to 8) range. Our results indicate that peats are characterised by a wide range of geohopanoids. However, the C_{31} hopane and C_{32} hopanoic acid (and occasionally the C_{32} hopanol) typically dominate. C_{32} hopanoic acids occur as αβ- and ββ-stereoisomers, with the ββ-isomer typically dominating. In contrast, C_{31} hopanes occur predominantly as the αβ-stereoisomer. These two observations collectively suggest that isomerisation is not inherited from an original biological precursor (i.e. biohopanoids). Using geohopanoid ββ/(αβ+ββ) indices, we demonstrate that the abundance of αβ-hopanoids is strongly influenced by the acidic environment, and we observe a significant positive correlation between C_{31} hopane isomerisation and pH (n = 94, r^2 = 0.64, $p < 0.001$). Crucially, there is no correlation between C_{31} hopane isomerisation and temperature. We therefore conclude that within peats, αβ-hopanoids are acid-catalysed diagenetic products and their occurrence at shallow

depths indicates that this isomerisation is rapid. This shows that geohopanoid ββ/(αβ+ββ) indices can be used to reconstruct pH within modern and ancient peat-forming environments. However, we only recommend using ββ/(αβ+ββ) indices to interrogate large amplitude (> 1 pH unit) and longer-term (> 1 kyr) variation. Overall, our findings demonstrate the potential of geohopanoids to provide unique new insights into understanding depositional environments and interpreting terrestrial organic matter sources in the geological record.

Highlights:

- Peats are characterised by a wide range of geohopanoids
- C_{32} hopanoic acids and C_{31} hopanes usually dominate the geohopanoid assemblage
- Diagenesis and isomerisation of geohopanoids occurs rapidly
- Hopane stereochemistry is strongly influenced by the acidic environment
- Geohopanoids may be a useful proxy for assessing relative changes in pH

Keywords: bacteria, hopanoids, peat, lignite, diagenesis, isomerisation

1 Introduction

Biohopanoids are pentacyclic triterpenoids produced by a wide range of bacteria (Pearson et al., 2007; Rohmer et al., 1984) and appear to perform a regulating and rigidifying function similar to sterols in eukaryotes (Kannenberg and Poralla, 1999; Sáenz et al., 2015). These compounds can be subdivided into two groups: simple hopanoids with a C_{30} ring system (e.g. diploptene/diplopterol) and complex hopanoids with an additional polyfunctionalised side chain (i.e. bacteriohopanepolyols (BHPs)). The latter can be unique markers for specific bacteria (Talbot and Farrimond, 2007) or certain environmental conditions (Bradley et al., 2010) and have been used to profile the bacterial community in terrestrial settings (Höfle et al., 2015; Talbot et al., 2016b). However, due to their polyfunctionalised side chain, BHPs are typically only preserved over relatively recent timescales (e.g. < 5 million years; Ma) (Handley et al., 2010; Schefuß et al., 2016; Talbot et al., 2014; Talbot et al., 2016b; Spencer-Jones et al., 2014; 2017) and their occurrence in much older sediments (e.g. the Paleocene-Eocene Thermal Maximum; 56 Ma) remains ambiguous (Talbot et al., 2016a).

Instead, reconstructions of the ancient bacterial community are more commonly based upon the abundance (Pancost et al., 2003), distribution (Birgel et al., 2006) and/or stable carbon isotopic composition (Inglis et al., 2015; Pancost et al., 2007) of their degradation products (i.e. geohopanoids). In sediments, with increasing diagenesis, geohopanoids undergo stereochemical transformations and the biologically-derived 17β,21β(H)-hopanoid is transformed into the more thermally stable 17β,21α(H) and 17α,21β(H)-stereoisomers (Mackenzie et al., 1980; Peters and Moldowan, 1991). With increasing maturation, extended hopanoids (>C_{30}) also undergo isomerisation at the C-22 position. Such changes have been widely used to reconstruct the thermal history of sediments (Farrimond et al., 1998; Mackenzie et

al., 1980; Peters and Moldowan, 1991; Seifert and Moldowan, 1980), where decreasing ββ/(αβ+ββ) indices and increasing 22S/(22R+22S) values indicate increasing thermal maturity.

However, whilst geohopanoids in modern sediments typically occur in the biological 17β,21β(H) configuration, in some modern peatlands the 'thermally mature' C_{31} 17α,21β(H)-homohopane (C_{31} αβ hopane, hereafter) dominates over the biological 17β,21β(H) isomer (Dehmer, 1993; Pancost et al., 2003; Quirk et al., 1984; Rohmer et al., 1984; Zhang et al., 2009). The predominance of the C_{31} αβ hopane in recent peat deposits which have not undergone thermal maturation could result from the direct input of αβ hopanoids by indigenous bacteria (Rosa-Putra et al., 2001). Alternatively, it could derive from oxidation and decarboxylation reactions of BHPs followed by isomerization at the C-17 position catalysed by the acidic environment (Pancost et al., 2003; Ries-Kautt and Albrecht, 1989). More recently, Huang et al. (2015) have argued that temperature and hydrology exert a control upon the formation of the C_{31} αβ hopane and it remains unclear why the C_{31} αβ hopane is so abundant in some peatlands. Such findings also complicate the application of geohopanoids as palaeoenvironmental proxies (see Pancost et al., 2003; McClymont et al., 2008; Inglis et al., 2015; Huang et al., 2015).

However, due to the small number of peats that have been studied as well as the lack of peatland diversity sampled, the environmental controls regulating geohopanoid distributions in peats remain poorly constrained. Here, we present the first global study of the occurrence, distribution and diagenesis of geohopanoids within peat using samples (n = 395) obtained from new and previously published datasets spanning a wide temperature (-1 to 27°C) and pH (3 to 8) range. Based upon this, we explore how the environment regulates hopanoid isomerisation in modern peatlands by comparing hopanoic acid and hopane ββ/(αβ+ββ) ratios to

129 both temperature and pH estimates. We then explore the utility of geohopanoids as
130 palaeoenvironmental indicators in natural archives.
131
132 **2. Methods**
133 2.1. Data compilation
134 Previously published C_{31} hopane ββ/(αβ+ββ) indices were obtained from the
135 Dajiuhu, Zoige, Hani, and Shiwangutian peatlands in China (Huang et al., 2015) (Fig.
136 1). These are surface samples collected from 0 to 2 cm depth (n = 63). For full
137 details on each site, see Huang et al. (2015). Previously published C_{31} hopane
138 ββ/(αβ+ββ) indices were also obtained from the Butterburn Flow (UK) peat
139 (McClymont et al., 2008). The samples were collected between 50 and 90cm depth
140 (n = 26). For full details on this site, see McClymont et al. (2008).

141 We also present unpublished C_{31} hopane ββ/(αβ+ββ) indices from Butterburn
142 Flow (n = 34; UK; Pancost et al., 2011), Bissendorfer Moor (n = 50; Germany;
143 Pancost et al., 2011), Ballyduff Bog (n = 50; Ireland; Pancost et al., 2011),
144 Kontolanrahka Bog (n = 45; Finland; Pancost et al., 2011) and Hongyuan (n = 26;
145 Tibet; Zheng et al., 2014). For each site (excluding Butterburn Flow) samples were
146 obtained between 0 and 100cm depth. At Butterburn Flow, samples were collected
147 between 0 and 50cm depth, and complement the dataset from McClymont et al.
148 (2008). The full experimental procedure for each site is described within the
149 supplementary information.

150
151 2.2. Sampling
152 To generate a global database of geohopanoid distributions, we analysed additional
153 samples (n = 111) from 23 wetlands in 9 different countries (Peru, Indonesia, Brazil,

USA, Argentina, Spain, Australia, Germany and Sweden; Fig. 1). Samples were obtained from peat cores spanning the upper 100 cm. The samples cover a broad range in mean annual temperature (MAAT) from -1 to 26°C. The peats are characterized by a wide variety of vegetation, ranging from *Sphagnum*-dominated ombrotrophic peats to *Cyperaceae*-dominated minerotrophic peats

2.3. Organic Geochemistry

2.3.1. Extraction and separation

Peats (n = 111) were extracted with an Ethos Ex microwave extraction system using 15 ml of dichloromethane (DCM) and methanol (MeOH) (9:1, *v/v*, respectively) at the Organic Geochemistry Unit in Bristol. The microwave program consisted of a 10min ramp to 70°C (1000 W), 10 min hold at 70°C (1000 W), and 20 min cool down. Samples were centrifuged at 1700 rounds per minute for 3-5 min, and the supernatant was removed and collected. A further 10 ml of DCM:MeOH (9:1, *v/v*) was added to the remaining peat material and centrifuged again, after which the supernatant was removed and combined with the previously obtained supernatant. This process was repeated 3-6 times, depending on the volume of sample, to ensure that all extractable lipids were retrieved. The TLE was initially separated over silica into apolar and polar fractions using hexane:dichloromethane (9:1, *v/v*) and dichloromethane:methanol (1:2, *v/v*), respectively. Due to an abundance of aromatic compounds within some apolar fractions, the apolar fractions were subsequently fractionated over silica into saturated hydrocarbon and aliphatic fractions using hexane (100%) and hexane:dichloromethane (3:1, *v/v*) respectively. Note that slightly different methodologies were used by Zheng et al. (2014) and Pancost et al. (2011), as well as for published data from Huang et al. (2015) and McClymont et al. (2008) (see Supplementary Information).

180

181 2.3.2. Methylation and silylation

182 For a subset of samples (35 out of 111), the polar fraction was methylated by adding
183 100µl of BF_3/MeOH and heating at 60°C for 30 minutes. The sample was cooled
184 down to room temperature before c. 1ml of DCM-extracted double distilled water was
185 added. This was followed by the addition of~ 2ml of DCM. The fatty acid methyl
186 esters were subsequently extracted from the bottom layer, added to a 7ml vial, and
187 the process was repeated twice. The sample was dried, redissolved in DCM and
188 eluted through an anhydrous sodium sulphate column to extract any residual water.
189 The column was washed through with DCM three times and the sample dried under
190 N_2 at 40°C. Prior to analysis, samples were silylated by adding 25µl of *N,O*-
191 bis(trimethylsilyl)trifluoroacetamide (BSTFA) and 25µl of pyridine, and heated for one
192 hour at 70°C. Samples were then allowed to cool and dried down under N_2. Silylated
193 samples were analysed by GC-MS within 24 h.

194

195 2.3.3. GC-MS analysis

196 Samples were analysed using a Thermo Scientific ISQ Single Quadrupole gas
197 chromatography-mass spectrometer (GC-MS). Using helium as the carrier gas, 1µl
198 of sample (dissolved in ethyl acetate) was injected at 70°C using an on-column
199 injector. The temperature program included four stages: 70°C hold for 1 min, 70-
200 130°C at 20°C/min rate; 130-300°C at 4°C/min; and temperature hold for 20 min at
201 300°C. The electron ionisation source was set at 70 eV. Scanning occurred between
202 *m/z* ranges of 50 to 650 Daltons. The GC was fitted with a fused silica capillary
203 column (50 m x 0.32 mm i.d.) coated with a ZB1 stationary phase
204 (dimethylpolysiloxane equivalent, 0.12 µm film thickness). Geohopanoids (see Fig.

A1) were identified based upon published spectra, characteristic mass fragments and retention times (e.g. Rohmer et al., 1984; Sessions et al., 2013; Uemura and Ishiwatari, 1995; Van Dorsselaer et al., 1974).

2.3.4. GC-C-IRMS analysis

GC-MS analysis revealed the occurrence of two unknown C_{30} hopenes (see section 3.1, 4.1 and supplementary information). To assess their potential origin, 15 hydrocarbon fractions from Bissendorfer Moor (Germany) were selected for compound specific stable carbon isotope ($\delta^{13}C$) analysis. These samples span the upper 100 cm and capture both the oxic acrotelm and anoxic catotelm. Gas chromatography-combustion-isotope ratio mass spectrometry (GC-C-IRMS) was performed using an Isoprime 100 GC-combustion-isotope ratio mass spectrometer system. Samples were measured in duplicate and $\delta^{13}C$ values were converted to VPDB by bracketing with an in-house gas (CO_2) of known $\delta^{13}C$ value. Instrument stability was monitored by regular analysis of an in-house standard. Injection volume was 1µl onto to a Zebron-I nonpolar column (50 m × 0.32 mm i.d., 0.10 µm film thickness). GC conditions were the same as described above for GC-MS analysis (see section 2.3.3.)

2.4. Environmental parameters

For each site, mean annual air temperature (MAAT) was calculated using the simple bioclimatic model PeatStash, which computes MAAT globally with a 0.5 degree spatial resolution (Gallego-Sala and Prentice, 2013; Naafs et al., 2017). PeatStash is preferred over (short-term) data from local weather stations as the spatial and temporal coverage of weather stations varies greatly across the globe. Published pH data were used as reported (see Charman et al, 2007, Zheng et al., 2014 and Huang

et al., 2015). For new sites, pH data were obtained from the literature or during sampling (Naafs et al., 2017).

2.5. Statistical analysis

To assess the role of environmental change upon hopanoid isomerisation ratios, we calculated Deming regressions using the R software package (http://www.R-project.org/). Deming regressions differ from simple linear regressions as they take into account the error on both the *x*- (e.g., proxy) and *y*-axis (e.g., environmental variable) (Adcock, 1878). Here, we assume that the error associated with proxy measurements and environmental parameters is independent and normally distributed. To calculate a Deming regression, we must define the standard deviation (σ) for both the *x*- and *y*-axis. For MAAT, the standard deviation is defined as 1.5°C (see Naafs et al., 2017). For pH, the standard deviation is defined as 0.5 pH units (see Naafs et al., 2017*).* For the C_{32} hopanoic acid and C_{31} hopane ββ/(αβ+ββ) indices, the standard deviation and ratio of variance must also be defined (see Supplementary Information). Residuals were calculated for the full dataset using the following equation:

$$Residual_y = y_{observed} - y_{predicted}$$

The root mean square error (RMSE) for *y*, was calculated using the following equation:

$$RSME_y = \sqrt{\frac{\sum_{x=1}^{n}(y_{x,observed} - y_{x,predicted})^2}{n} \times \frac{n}{df}}$$

Where *df* stands for degrees of freedom, which in this case is n-1.

To assess the interdependence of temperature and pH upon hopane isomerisation ratios, we also constructed x-y plots of temperature and pH and plotted C_{31} ββ/(αβ+ββ) ratios as a third continuous variable (Fig. A2).

3. Results

3.1. Geohopanoid distributions

In our global dataset, most samples come from strongly acidic peats with pH < 5 (n = 278 samples from 22 settings); however, the data set includes peats from moderately acidic (pH 5 to 7) and neutral-to-slightly alkaline (pH > 7) peatlands (78 samples from 13 settings and 22 samples from 4 settings, respectively). Within the global dataset, the hydrocarbon fraction contained a range of C_{27} to C_{32} hopanes and C_{27} to C_{30} hopenes (Fig. 2a). Hopanes and/or hopenes were detected in 378 out of 395 samples. The dominant hopanoid in the hydrocarbon fraction was typically the (22R)-17α,21β(H)-homohopane (C_{31}) (Fig. 2a). However, in some settings 17β(H)-trisnorhopane (C_{27}), hop-22(29)-ene (C_{30}; diploptene) or two C_{30} hopenes with unknown structures dominated the hydrocarbon fraction. The latter are characterised by a molecular ion of *m/z* 410 with a base peak of *m/z* 191, major ions at *m/z* 69, 81, 95, 189 and minor ions at *m/z* 395 (Fig. A3). The hydrocarbon fraction was also characterized by a range of minor compounds, including: 17,21-epoxyhopane, 17α(H)- and 17β(H)-trisnorhopane (C_{27}), 17α,21β(H)- and 17β,21β(H)-norhopane (C_{29}), 17α,21β(H)-, 17 β,21α(H)- and 17β,21β(H)-hopane (C_{30}), (22S)-17α,21β(H)-, (22R)-17β,21α(H)- and -17β,21β(H)-homohopane (C_{31}), 17β,21β(H)-bishomohopane (C_{32}), 22,29,30-Trisnorhop-17(21)-ene (C_{27}), Hop-17(21)-ene (C_{30}) and 2-methylhop-17(21)-ene (C_{31}) (See Fig. 2a and Fig. A1).

Within the polar fractions, the dominant compound in most settings was 17β,21β(H)-bishomohopanoic acid (C_{32}) (Fig. 2b). 17α,21β(H)-bishomohopanoic acid (C_{32}) was also relatively abundant. In addition to these major compounds, the polar fraction was characterized by a range of other hopanoids, including: hopan-29-ol (C_{30}; diplopterol), 17β,21β(H)-homohopanoic acid (C_{31}), 17β,21α(H)-bishomohopanoic acid (C_{32}), 17β,21β(H)-bishomohopanol (C_{32}), 17β,21α(H)-trishomohopanoic acid (C_{33}) and 17β,21β(H)-trishomohopanoic acid (C_{33}) (Fig. 2b).

3.2. Geohopanoid isomerisation ratios

The degree of geohopanoid isomerisation was assessed using ββ/(αβ+ββ) and 22S/(22S+22R) indices (MacKenzie et al., 1980). The global average C_{31} hopane ββ/(αβ+ββ) is relatively low with an average value of 0.23 (n = 378, σ = 0.26; Fig. A4). In contrast, C_{32} hopanoic acid ββ/(αβ+ββ) values were relatively high with an average value of 0.75 (n = 35, σ = 0.19; Fig. A5). In the majority of *Sphagnum* (Fig. 3) and non-*Sphagnum* dominated peatlands (Fig. 4), downcore C_{31} hopane ββ/(αβ+ββ) indices remain stable or slightly decrease with depth. Within a sub-set of our dataset, we also obtained C_{31} 22S/(22S+22R) indices. As values were low and stable throughout (average = 0.04, n = 106, σ = 0.06), we did not revisit older studies.

3.3. Geohopanoid $\delta^{13}C$ values

$\delta^{13}C$ values were determined for 15 samples within Bissendorfer Moor, Germany, where two unknown C_{30} hopenes comprise 30-40% of the hopane/hopene assemblage. The earlier eluting C_{30} hopene $\delta^{13}C$ value ranges from -24.9 to -29.9‰ (average: -27.5‰), whereas that of the later eluting C_{30} hopene is more depleted and ranges from -26.5 to -34.7‰ (average: -29.7‰). Both values are ^{13}C-depleted (ca. 3-

6‰ lower) compared to the C_{31} αβ hopane (average: -24.6 ±1.0‰) and C_{31} ββ hopane (average: -23.2 ±1.7‰) for a given sample. For comparison, $\delta^{13}C$ values from higher plant- (C_{29} to C_{33} *n*-alkanes) and eukaryote- (5α-Cholestane) biomarkers in these samples are -33.9 ± 0.3 ‰ and -25.7 ± 0.1 ‰, respectively.

4. Discussion

4.1. Geohopanoid distributions in modern peats

Previous studies indicate that peatlands contain a diverse range of geohopanoids (Quirk et al., 1984; Pancost et al., 2003; Zhang et al., 2009; Huang et al., 2015). However, our global dataset indicates that geohopanoid distributions are typically dominated by the C_{32} ββ hopanoic acid (Fig. 2.b) and C_{31} αβ hopane (Fig. 2.a). This is consistent with previous studies (e.g. Quirk et al., 1984; Ries-Kautt and Albrecht, 1989; Dehmer, 1993; Pancost et al., 2003; Huang et al., 2015; Chaves-Torres and Pancost, 2016). Also in agreement with previous observations (e.g. Dehmer, 1993; Pancost et al., 2003; Quirk et al., 1984), the C_{31} αβ hopane dominates the hopane distribution within acidic (pH < 6), ombrotrophic and *Sphagnum*-dominated peats. In other settings, diploptene is the dominant compound. However, it is found across a wide pH (ca. 3 to 8) and temperature range (-1 to 26°C), suggesting it is not restricted in its occurrence (c.f. C_{31} αβ hopane). This is consistent with the fact that diploptene is synthesised by a wide variety of aerobic (Rohmer et al., 1984) and also anaerobic bacteria (Härtner et al., 2005; Sinninghe Damsté et al., 2004).

We also report the occurrence of two unknown C_{30} hopenes within six *Sphagnum*-dominated bogs (see Supplementary Information and Fig. A3). To explore the source of these compounds further, we determined the carbon isotopic composition of these compounds within Bissendorfer Moor (Germany). The C_{30} hopenes are ^{13}C-depleted (ca. 3-6‰) relative to C_{31} hopanes at Bissendorfer Moor

and likely derive from bacterial sources consuming a diverse suite of carbon substrates (see Pancost et al., 2003; Inglis et al., 2015). This includes ^{13}C-enriched carbohydrates but also more ^{13}C-depleted organic matter or even methane-derived CO_2. This is consistent with the BHP distribution in Bissendorfer Moor which is dominated by bacteriohopanetetrol, bacteriohopanetetrol cyclitol ether and 35-aminobacteriohopane-32,33,34-triol (i.e. saturated tetrafunctionalised BHPs; Talbot et al., 2016; van Winden et al., 2012a; van Winden et al., 2012b; Kim et al., 2011), suggesting a largely heterotrophic bacterial community with only some evidence for aerobic methanotrophy (Talbot et al., 2016b).

4.2. Diagenesis of geohopanoids in peats

Our results indicate that peatlands are dominated by a range of geohopanoids including hopanoic acids, hopanols, hopanes and hopenes. These compounds can be directly biosynthesised (i.e. diploptene) or derived from BHPs. Although we have not analysed BHPs here, based on previous work (Talbot et al., 2016b) it is likely that they are also widespread. However, the diagenesis of bio- and geohopanoids remains poorly constrained. Whilst most BHPs can be preserved to significant depth (>400 cm) within peatlands, there can be a significant decrease in the concentration of unsaturated BHPs (e.g. unsaturated BHT-pentose) and “soil-marker BHPs” (e.g. adenosylhopane) below the upper surface layer of a *Sphagnum*-dominated bog. This is likely related to diagenesis under highly acidic conditions (e.g. Talbot et al., 2016).

BHPs also undergo oxidative degradation to form a range of degradation products, including hopanoic acids and hopanols (Adam et al., 2016; Bisseret and Rohmer, 1995; Farrimond et al., 2003; Innes et al., 1997; Quirk et al., 1984). Within peat-forming environments, tetrafunctionalised BHPs are associated with the presence of C_{32} hopanoic acids (Innes et al., 1997; Ries-Kautt and Albrecht, 1989).

This suggests that diagenesis is analogous to periodic acid/sodium borohydride treatment (i.e. 1,2-diol cleavage), whereby oxidative cleavage of vicinal diols (**1**) gives access to an intermediate C_{32} hopanoid aldehyde (**9**) before undergoing oxidation to form the C_{32} hopanoic acid (**10**) (Bisseret and Rohmer, 1995; Peiseler and Rohmer, 1991; Zundel and Rohmer, 1985). This model is also consistent with the low abundance of penta- and hexafunctionalised BHPs and C_{31} and C_{30} hopanoic acids in peat (Talbot et al., 2016b; *this paper*). Here, we show for the first time that the dominance of C_{32} hopanoic acids in peat is global, suggesting that tetrafunctionalised BHPs dominate within a range of diverse peat-forming environments. It also suggests that similar diagenetic processes are occurring on a global scale.

Previous studies proposed that decarboxylation of the C_{32} hopanoic and/or dehydration of the C_{32} hopanol then yields the C_{31} hopane (Barton et al., 1980; Bennett and Abbott, 1999). Based upon the high abundance of C_{32} hopanoic acids in peat, we suggest that decarboxylation of the C_{32} hopanoic acid **(10-11)** (rather than dehydration of the C_{32} hopanol) is the primary source of the C_{31} hopane **(16-17)** in peat (Fig. 5). This is consistent with Huang et al (2015) who have shown a statistically significant correlation ($p < 0.01$) between C_{32} hopanoic acid and C_{31} hopane concentrations within a Chinese peatland.

Crucially, we show that bio- and geohopanoid diagenesis occurs rapidly in peatlands and geohopanoids are detected within the upper 0-5 cm of many peats. Geohopanoid concentrations usually remain low within the upper oxic layer (< 20 cm; Fig. 6), although there are some exceptions (e.g. Kontolanrahka Bog, Finland). Geohopanoid concentrations are substantively higher at the oxic/anoxic boundary (ca. 20-40 cm in our peats; Fig. 6). As hopanoids are predominantly, although not exclusively, derived from aerobic bacteria, this increase is attributed to microbial

decomposition and/or transformation of BHPs (Innes et al., 1998; Torres and Pancost, 2016). Below the oxic/anoxic boundary, geohopanoid concentrations are rather variable (Fig. 6), suggesting that additional diagenesis may occur at depth (see also Chaves-Torres, 2015).

Our results also indicate that C_{32} hopanoic acids and C_{32} hopanols occur as αβ- and ββ-stereoisomers in peat, with the ββ-isomer typically dominating (Fig. 2b). In contrast, the C_{31} hopane occurs predominantly as the αβ-stereoisomer (Fig. 2a). An offset between hopanoic acid and hopane isomerisation ratios has been observed in Mesozoic sediments (Schaeffer et al. 1993; Bennett and Abbott, 1999; Farrimond et al. 2002), where isomerisation is suppressed for increasingly functionalised compounds (e.g. hopanoic acids and hopanols). Indeed, this may explain the lack of αβ-BHPs in modern peats (Talbot et al., 2016b). We also show that isomerisation occurs rapidly, and αβ hopanes often dominate within the top 5 cm of peatlands (Fig. 3-4). This suggests that ββ/(αβ+ββ) ratios in peat are likely set during early diagenesis. However, there can be a subtle decrease in ββ/(αβ+ββ) ratios with depth (Fig. 3-4), suggesting further isomerisation of geohopanoids may occur below the acrotelm/catotelm boundary (see also 4.3)

4.3. Environmental controls on geohopanoid isomerization in peat

Our results indicate that C_{32} hopanoic acids and C_{31} hopanes occur in the αβ-configuration, with a particularly high abundance of the latter. However, it remains unclear why αβ-isomers are so abundant in modern peat. Previous studies have suggested αβ geohopanoids could derive from the direct input of 17α,21β(H)-hopanoids by indigenous bacteria (e.g. Huang et al., 2015). Indeed, Rosa-Putra et al. (2001) reported the presence of 17α,21β(H)- and 17β,21α(H)-biohopanoids alongside the more common ββ isomer in some *Frankia* spp. (Actinobacteria; n.b.

411 the relative abundance of these compounds is unknown). Although Actinobacteria
412 are an important phyla within the peat microbiome (e.g. Dedysh et al., 2006), all
413 biohopanoids observed in modern peatlands occur as a single 17β,21β(H)- isomer
414 (Kim et al., 2011; Talbot et al., 2016b; van Winden et al., 2012). This is true even for
415 early diagenetic intermediate hopanepolyols derived from the degradation of BHPs
416 including: tetrakishomohopane-32,33,34-triol and trishomohopane-32,33-diol (e.g.
417 Rodier et al., 1999; Watson and Farrimond, 2000). The fact that hopanes exhibit a
418 greater degree of isomerisation than functionalised bio- and geohopanoids, their
419 putative precursors, suggests that isomerisation is not inherited from original
420 biological sources. As such, we argue that biosynthesis of αβ-hopanoids is unlikely
421 to directly account for the majority of αβ geohopanoids in peat.
422 Instead, the occurrence of the C_{31} αβ hopane has been ascribed to acid-
423 catalysed isomerisation (Ries-Kautt and Albrecht, 1989). To explore this further, we
424 compared hopanoic acid and hopane ββ/(αβ+ββ) indices to pH within our global
425 dataset. For sites with only a single pH measurement, we report the average
426 ββ/(αβ+ββ) value (Fig. 7). Both C_{32} hopanoic acid and C_{31} hopane ββ/(αβ+ββ) ratios
427 exhibit a linear positive correlation with pH. The correlation between the C_{31} hopane
428 ββ/(αβ+ββ) index and pH is statistically significant ($r^2 = 0.64$, $p < 0.001$; $n = 94$; Fig.
429 7a), indicating that pH exerts a first-order control upon hopane isomerisation in
430 peats. In contrast, the correlation between C_{32} hopanoic acid ββ/(αβ+ββ) indices and
431 pH is not statistically significant ($r^2 = 0.13$; $n = 20$; $p = 0.11$ Fig. 7b) and ratios are
432 higher and less variable across the sample set. These features could arise from
433 sedimentary diagenetic constraints. For example, the weak ionic adsorption of
434 functionalised compounds to mineral surfaces could inhibit isomerisation (Farrimond
435 et al., 2002). Farrimond et al. (2002) have also shown that decarboxylation can
436 promote isomerisation through bond cleavage and may explain why the C_{31} hopane

437 isomerisation ratio exhibits a stronger relationship with pH; thus, it might be the
438 decarboxylation step that is crucial to the signal preserved in hopanes.
439 More recently, Huang et al. (2015) argued that temperature exerts a control
440 upon hopane isomerisation, with enhanced formation of αβ-geohopanoids in warmer
441 settings. However, this conclusion was based upon a single site with a relatively
442 complex evolution history. To explore this further, we compared hopanoic acid and
443 hopane ββ/(αβ+ββ) indices to MAAT within our global dataset. Here, we report the
444 average ββ/(αβ+ββ) value for a given site (Fig 8; see Supplementary Information).
445 Our results reveal no correlation between C_{31} hopane ββ/(αβ+ββ) indices and MAAT
446 ($r^2 = 0.01$, $p = 0.55$; $n = 35$; Fig. 8b). X-Y plots of temperature and pH with C_{31}
447 ββ/(αβ+ββ) ratios as a third continuous variable support this observation (Fig. ~~A~~3).
448 Our results also indicate no correlation between C_{32} hopanoic acid ββ/(αβ+ββ)
449 indices and temperature ($r^2 = 0.09$, $p = 0.19$, $n = 20$, Fig. 8a). We attribute this
450 discrepancy to the fact that Huang et al. (2015) utilise a downcore paleo-temperature
451 record, where temperature variations are inferred rather than directly measured.
452 Huang et al. (2015) also argue that hydrological conditions impact geohopanoid
453 isomerisation, with enhanced formation of αβ hopanoids under drier conditions.
454 However, hydrology and pH can be closely linked within peat-forming environments
455 (e.g, Zhong et al., 2017) and extensive rainfall can result in dilution, decreased
456 acidity and a reduction in the formation of αβ-hopanoids (e.g. Pancost et al., 2003).
457 To characterise the impact of hydrology upon hopanoid distributions, future studies
458 should utilise a setting with minor variations in temperature and pH, but large
459 changes in moisture content (c.f. Dang et al. 2016).
460 There may also be other factors which influence hopanoid isomerisation ratios.
461 For example, Quirk et al. (1984) have argued that vegetation type promotes the
462 formation of αβ hopane. This is based upon an increase in the relative abundance of

the C_{31} αβ hopane in a series of *Sphagnum* decay experiments (Quirk, 1978). While this is possible, it does not explain why αβ-hopanoids are rapidly formed in non-*Sphagnum* settings and high acidity seems to be necessary. Likewise, Huang et al. (2015) have suggested that total organic carbon (TOC) content could be important, with enhanced production of αβ-hopanoids in high TOC settings (e.g. Gong et al., 2015; Huang et al., 2015). However, this does not explain why ββ-hopanoids dominate in some high TOC settings. Again, high acidity seems to be required.

4.4. Geohopanoids as palaeoenvironmental proxies

Our results support the original hypothesis of Quirk et al. (1984), which suggests that the formation of the αβ hopanoids in peats is strongly dependent on pH. Crucially, isomerisation appears to be fixed during early diagenesis, suggesting that geohopanoid ββ/(αβ+ββ) indices could be a useful proxy for understanding pH over a range of timescales. Here, we utilise the C_{31} hopane ββ/(αβ+ββ) index to construct a peat-specific hopane-based pH proxy:

$$pH = 5.22 * (C_{31}\text{ hopane } \beta\beta/\alpha\beta+\beta\beta) + 3.11 \quad (n=94,\ r^2 = 0.64,\ RMSE = 1.4)$$

The coefficient of correlation is stronger than obtained from other peat-specific pH proxies (e.g. the cyclisation of branched glycerol dialkyl glycerol tetraethers (*br*GDGTs); $r^2 = 0.58$, Naafs et al., 2017); however, the RMSE is larger than previously found for *br*GDGTs (see Naafs et al., 2017). Hopane-derived pH estimates were also compared to *br*GDGT-derived pH estimates (CBT_{peat}; Naafs et al., 2017) from the same sample set (Fig. A6). Although the correlation deviates from the 1:1 line - indicating that C_{31} ββ/αβ+ββ ratios give lower pH estimates compared to those obtained using brGDGTs for a given sample - there is a statistically

489 significant correlation between CBT_{peat} and C_{31} ββ/αβ+ββ-based pH values ($p < 0.01$; $r^2 = 0.43$; Fig. A6).

491 To explore the utility of ββ/(αβ+ββ) indices in natural archives, we calculated
492 downcore pH profiles for each site in our global dataset. All sites exhibit relatively
493 constant pH values within the upper 100cm and are consistent with relatively stable
494 climate conditions over the last millennium (Crowley, 2000). The only exception is
495 Bissendorfer Moor (Germany), which exhibits a significant decrease in pH (ca. 4 pH
496 units) within the upper 30cm. However, as the hydrology of this site has been
497 strongly affected by artificial drainage, the surface microbial community may have
498 been affected by human activity (see Talbot et al., 2016).

499 It is also possible to calculate pH estimates from previously published
500 datasets. For example, Pancost et al. (2003) observed a subtle increase in
501 ββ/(αβ+ββ) ratios within the Bargerveen peat core during the Sub-Boreal/Sub-
502 Atlantic transition (ca. 2800 years ago; Pancost et al., 2003). This was originally
503 attributed to decreasing acidity (due to enhanced precipitation) and is consistent with
504 our results which indicate a clear pH control on the degree of C_{31} hopane
505 isomerisation. Hopane-derived pH estimates are also relatively low (ca. 3.5)
506 throughout the peat core and consistent with the abundance of *Sphagnum* moss in
507 the peat (Pancost et al., 2003). However, the magnitude of pH change across the
508 Sub-Boreal/Sub-Atlantic transition is relatively minor (0.2 pH units) and within the
509 error of this proxy. Therefore, we only recommend using ββ/(αβ+ββ) indices to
510 interrogate large amplitude and more long-term pH variation (see below). It is also
511 important to note that the composition of the bacterial community will likely vary
512 between environments (e.g. Dedysh et al., 2006; Bragina et al., 2012; Serkebaeva et
513 al., 2013; Lin et al. 2012). Such changes are likely to impact hopanoid distributions

514 and perhaps isomerisation ratios; however, this is hard to deconvolve and requires
515 further investigation.
516 The C_{31} ββ/(αβ+ββ) index could also be applied to immature coal deposits
517 (i.e. lignites) to understand environmental change during past greenhouse periods
518 and across hyperthermal events. To explore this, we assessed the geohopanoid
519 distribution within a thermally immature, early Paleogene (~56 Ma) lignite deposit
520 (Schöningen, Germany). Within this setting, the C_{31} αβ isomer dominates the hopane
521 assemblage, suggesting an acidic (pH <6), ombrotrophic peatland (Fig. 9). This is
522 consistent with the occurrence of *Sphagnum*-type spores and biomarkers within this
523 lignite seam (Inglis et al., 2015; Inglis et al., 2017). Intriguingly, hopane-derived pH
524 values (ca. 4.9) are similar to the average value of 5.0 derived from branched
525 GDGTs (CBT_{peat}; Naafs et al., 2017). Both proxies also exhibit similar temporal
526 trends, although the magnitude of the variations exhibited by the former are larger
527 (Fig. 9).
528 We have previously suggested that low C_{31} ββ/(αβ+ββ) indices could also be
529 a useful proxy to trace the input of acidic peat (or eroded lignite) to marine or fjord
530 sediments (Inglis et al., 2015; Smittenberg et al., 2004). While our results generally
531 support this hypothesis, some acidic peats exhibit relatively high C_{31} ββ/(αβ+ββ)
532 indices (e.g. Brazil), dictating caution in this approach – in particular, an absence of
533 substantive αβ-hopane inputs should not be interpreted as evidence for an absence
534 of peat inputs. As such, additional lines of evidence should be utilised to trace the
535 input of acidic peat into marine and/or lake sediments (e.g. *Sphagnum* biomarkers
536 and/or *Sphagnum* macrofossils (McClymont et al., 2011; Nichols and Huang, 2007;
537 Nott et al., 2000).
538 Finally, the ββ/(αβ+ββ) index could also provide insights into pH within other
539 environmental settings. For example, there is a significant correlation between C_{32}

hopanoic acid ββ/(αβ+ββ) ratios and pH in a suite of geothermal sinters (pH: from 2.5 to 9.0; r^2 = 0.85) (Pancost et al., 2006). However, interpretation of such ratios in older sinters will be more problematic as both temperature and pH, as well as extent of exposure to each of these, will have to be considered.

5. Conclusions

Using >350 samples spanning a wide temperature (-1 to 27°C) and pH (3 to 8) range, we have assessed the environmental controls regulating geohopanoid distributions in peats. Our results indicate that peats are characterised by a range of geohopanoids; however, C_{32} hopanoic acids and C_{31} hopanes typically dominate. C_{32} hopanoic acids and C_{31} hopanes both occur in the αβ-configuration and can form almost instantaneously in peatlands (i.e. within the upper 5 cm). This process appears to be strongly regulated by the acidic environment. In particular, the C_{31} hopane isomerisation ratio exhibits a statistically significant correlation with pH. Crucially, there is no correlation between C_{31} hopane isomerisation and temperature. Therefore, our study supports the hypothesis that within peatlands, αβ-hopanoids are acid-catalysed degradation products. This finding suggests that geohopanoid ββ/(αβ+ββ) indices could be used to reconstruct pH within modern and ancient peat-forming environments. Furthermore, we envisage that geohopanoids can provide important new insights into understanding depositional environments and interpreting terrestrial organic matter sources in the geological record.

6. Acknowledgements

This research was funded through the advanced ERC grant ‘The Greenhouse Earth System’ (T-GRES. Project reference: 340923). RDP acknowledges the Royal Society Wolfson Research Merit Award. YZ thanks the National Natural Science

Foundation of China (Project reference: 41372033). ELM acknowledges the Philip Leverhulme Prize. We also thank the NERC Life Sciences Mass Spectrometry Facility (Bristol) for analytical support and D. Atkinson for help with the sample preparation. GNI thanks Janet Dehmer and Philippe Schaeffer for helpful discussions. Members of the T-GRES Peat Database collaborators are M.J. Amesbury, H. Biester, R. Bindler, J. Blewett, M.A. Burrows, D. del Castillo Torres, F.M. Chambers, A.D. Cohen, S.J. Feakins, M. Gałka, A. Gallego-Sala, L. Gandois, D.M. Gray, P.G. Hatcher, E.N. Honorio Coronado, P.D.M. Hughes, A. Huguet, M. Könönen, F. Laggoun-Défarge O. Lähteenoja, M. Lamentowicz, R. Marchant, X. Pontevedra-Pombal, C. Ponton, A. Pourmand, A.M. Rizzuti, L. Rochefort, J. Schellekens, F. De Vleeschouwer. Finally, we thank Darci Rush, Phil Meyers and an anonymous reviewer for their comments and thoughtful suggestions which greatly improved this manuscript.

7. Figure captions

Figure 1: Map with the location of all peats used in this study. New and unpublished data shown in red. Previously published data is shown in orange (for interpretation of the references to colour in this figure legend, the reader is referred to the web version of this article).

Figure 2: Partial *m/z* 191 gas chromatogram of a typical (a) hydrocarbon and (b) polar fraction. Numbers accompanied with Greek letters signify the carbon number and stereochemistry of hopanoids.

Figure 3: Downcore C_{31} hopane ββ/αβ+ββ profiles for *Sphagnum*-dominated peatlands. a) Germany (Bissendorfer Moor), b) Ireland (Ballyduff Bog), c) Finland (Kontolanrahka Bog), d) UK (Butternburn Flow), e) Germany (Odersprung Bog), f) Argentina (Tierra del Fuego)

Figure 4: Downcore C_{31} hopane ββ/αβ+ββ profiles for non-*Sphagnum* peatlands. a) Indonesia (Sebangau), b) Brazil (Pinhieros), c) Spain (Zalama),d) Tibet (Hongyuan), e) Australia (Bomfield Swamp)

Figure 5: Proposed steps in the diagenesis of bio- and geohopanoids in peat. The structures in red were identified in modern peats. The structure in blue corresponds to a postulated intermediate. For interpretation of the references to hopanoids in this figure, the reader is referred to the supplementary information. (for interpretation of the references to colour in this figure legend, the reader is referred to the web version of this article).

Figure 6: Geohopanoid abundance with depth. a) Ballyduff Bog (Ireland), b) Butterburn Flow (Great Britain), c) Kontolanrahka Bog (Finland) and d) Bissendorfer Moor (Germany). Anoxic catotelm denoted in dark grey. n.b. the polar fraction was not methylated; as such, hopanoic acids were not GC-amenable under standard conditions and only hopanols were analysed here.

Figure 7: Impact of pH upon geohopanoid isomerisation. a) C_{31} hopane ββ/αβ+ββ index vs pH, b) C_{32} hopanoic acid ββ/αβ+ββ index vs pH

Figure 8: Impact of temperature upon geohopanoid isomerisation. a) C_{31} hopane ββ/αβ+ββ index vs MAAT, b) C_{32} hopanoic acid ββ/αβ+ββ index vs MAAT

Figure 9: pH and vegetation change within Seam 1, Schöningen during the latest Paleocene and/or earliest Eocene. a) the C_{31} hopane ββ/αβ+ββ index, b) C_{31} hopane ββ/αβ+ββ-derived pH estimates, c) CBT_{peat}-derived pH estimates (Naafs et al., 2017), d) C_{23}/C_{31} *n*-alkane ratio (i.e. proxy for input of *Sphagnum* moss; Inglis et al., 2015), e) the relative abundance (total palynomorphs) of *Sphagnum*-type spores (Inglis et al., 2015). Zero depth marks the top of seam 1 and the base of the overlying marine interbed 2 (for interpretation of the rFeferences to colour in this figure legend, the reader is referred to the web version of this article).

References

Adam, P., Schaeffer, P., Schmitt, G., Bailly, L., Courel, B., Fresnais, M., Fossurier, C. and Rohmer, M. (2016) Identification and mode of formation of hopanoid nitriles in archaeological soils. *Org. Geochem.* **91**, 100-108.

Barton, D.H., Dowlatshahi, H.A., Motherwell, W.B. and Villemin, D. (1980) A new radical decarboxylation reaction for the conversion of carboxylic acids into hydrocarbons. *Journal of the Chemical Society, Chemical Communications*, 732-733.

Bennett, B. and Abbott, G.D. (1999) A natural pyrolysis experiment — hopanes from hopanoic acids? *Org. Geochem.* **30**, 1509-1516.

Birgel, D., Thiel, V., Hinrichs, K.-U., Elvert, M., Campbell, K.A., Reitner, J., Farmer, J.D. and Peckmann, J. (2006) Lipid biomarker patterns of methane-seep microbialites from the Mesozoic convergent margin of California. *Org. Geochem.* **37**, 1289-1302.

Bisseret, P. and Rohmer, M. (1995) From bio- to geohopanoids: an efficient abiotic passage promoted by oxygen in the presence of cuprous chloride. *Tetrahedron Lett.* **36**, 7077-7080.

643 Bradley, A.S., Pearson, A., Sáenz, J.P. and Marx, C.J. (2010) Adenosylhopane: The first
644 intermediate in hopanoid side chain biosynthesis. *Org. Geochem.* **41**, 1075-1081.
645 Bragina, A., Berg, C., Cardinale, M., Shcherbakov, A., Chebotar, V. and Berg, G (2012)
646 Sphagnum mosses harbour highly specific bacterial diversity during their whoole
647 lifecycle. *ISME J*. **6.** 802-813
648 Charman, D.J., Blundell, A. and ACCROTELM members (2007) A new European testate
649 amoebae transfer function for palaeohydrolgical reconstruction on ombrotrophic
650 peatlands. *J. Quat. Sci.* **22**. 209-221
651 Crowley, T.J (2000) Causes of Climate Change Over the Past 1000 Years. *Science*. **289**. 270-
652 277
653 Dang, X., Yang, H., Naafs, B.D.A., Pancost, R.D and Xie, S (2016) Evidence of moisture
654 control on the methylation of branched glycerol dialkyl glycerol tetraethers in semi-arid
655 and arid soils. G*eochim. Cosmochim. Acta*. **189**. 24-36
656 Dedysh, S.N., Pankratov, T.A., Belova, S.E., Kulichevskaya, I.S. and Liesack, W. (2006)
657 Phylogenetic Analysis and In Situ Identification of Bacteria Community Composition in
658 an Acidic Sphagnum Peat Bog. *Appl. Environ. Microbiol.* **72**, 2110-2117.
659 Dehmer, J. (1993) Petrology and organic geochemistry of peat samples from a raised bog in
660 Kalimantan (Borneo). *Org. Geochem.* **20**, 349-362.
661 Farrimond, P., Griffiths, T. and Evdokiadis, E. (2002) Hopanoic acids in Mesozoic sedimentary
662 rocks: their origin and relationship with hopanes. *Org. Geochem.* **33**, 965-977.
663 Farrimond, P., Love, G.D., Bishop, A.N., Innes, H.E., Watson, D.F. and Snape, C.E. (2003)
664 Evidence for the rapid incorporation of hopanoids into kerogen. *Geochim. Cosmochim.*
665 *Acta* **67**, 1383-1394.
666 Farrimond, P., Taylor, A. and TelnÆs, N. (1998) Biomarker maturity parameters: the role of
667 generation and thermal degradation. *Org. Geochem.* **29**, 1181-1197.
668 Gallego-Sala, A.V. and Prentice, I.C. (2013) Blanket peat biome endangered by climate
669 change. *Nat. Clim. Change* **3**, 152-155.
670 Handley, L., Talbot, H.M., Cooke, M.P., Andersoon, K.E. and Wagner, T. (2010)
671 Bacteriohopanepolyols as tracers for continental and marine organic matter supply and

672 phases of enhanced nitrogen cycling on the late Quaternary Congo deep sea fan. *Org.*
673 *Geochem.* **41**. 910-914
674 Härtner, T., Straub, K.L. and Kannenberg, E. (2005) Occurrence of hopanoid lipids in
675 anaerobic Geobacter species. *FEMS Microbiol. Lett.* **243**, 59-64.
676 Höfle, S.T., Kusch, S., Talbot, H.M., Mollenhauer, G., Zubrzycki, S., Burghardt, S. and
677 Rethemeyer, J. (2015) Characterisation of bacterial populations in Arctic permafrost
678 soils using bacteriohopanepolyols. *Org. Geochem.* **88**, 1-16.
679 Huang, X., Meyers, P.A., Xue, K., Gong, L., Wang, X and Xie, S (2015) Environmental factors
680 affecting the low temperature isomerization of homohopanes in acidic peat deposits.
681 *Geochim. Cosmochim. Acta.* **154**. 212-228
682 Inglis, G.N., Collinson, M.E., Riegel, W., Wilde, V., Robson, B.E., Lenz, O.K. and Pancost,
683 R.D. (2015) Ecological and biogeochemical change in an early Paleogene peat-
684 forming environment: Linking biomarkers and palynology. *Palaeogeogr.*
685 *Palaeoclimatol., Palaeoecol.* **438**, 245-255.
686 Inglis, G.N., Collinson, M.E., Riegel, W., Wilde, V., Farnsworth, A., Lunt, D.J., Valdes, P.,
687 Robson, B.E., Scott, A.C., Lenz, O.K., Naafs, B.D.A and Pancost, R.D (2017) Mid-
688 latitude continental temperatures through the early Eocene in western Europe. *Earth*
689 *Planet. Sci. Lett.* **460**. 86-96
690 Innes, H.E., Bishop, A.N., Fox, P.A., Head, I.M. and Farrimond, P. (1998) Early diagenesis of
691 bacteriohopanoids in recent sediments of Lake Pollen, Norway. *Org. Geochem.* **29**,
692 1285-1295.
693 Innes, H.E., Bishop, A.N., Head, I.M. and Farrimond, P. (1997) Preservation and diagenesis
694 of hopanoids in recent lacustrine sediments of Priest Pot, England. *Org. Geochem.*
695 **26**, 565-576.
696 Kannenberg, E.L. and Poralla, K. (1999) Hopanoid biosynthesis and function in bacteria.
697 *Naturwissenschaften* **86**, 168-176.
698 Kim, J.H., Talbot, H.M., Zarzycka, B., Bauersachs, T. and Wagner, T. (2011) Occurrence and
699 abundance of soil-specific bacterial membrane lipid markers in the Têt watershed

(southern France): Soil-specific BHPs and branched GDGTs. *Geochem. Geoph. Geosy.* **12**.

Lin, X., Green, S., Tfaily, M.M., Prakash, O., Konstantinidis, K.T., Corbett, J.E., Chanton, J.O., Cooper, W.T and Kostka, J.E (2012) Microbial Community Structure and Activity Linked to Contrasting Biogeochemical Gradients in Bog and Fen Environments of the Glacial Lake Agassiz Peatland. *Appl. Environ. Microbiol.* 78**.** 7023-7031

Mackenzie, A., Patience, R., Maxwell, J., Vandenbroucke, M. and Durand, B. (1980) Molecular parameters of maturation in the Toarcian shales, Paris Basin, France—I. Changes in the configurations of acyclic isoprenoid alkanes, steranes and triterpanes. *Geochim. Cosmochim. Acta* **44**, 1709-1721.

McClymont, E.L., Bingham, E.M., Nott, C.J., Chambers, F.M., Pancost, R.D. and Evershed, R.P. (2011) Pyrolysis GC–MS as a rapid screening tool for determination of peat-forming plant composition in cores from ombrotrophic peat. *Org. Geochem.* **42**, 1420-1435.

McClymont, E.L., Mauquoy, D., Yeloff, D., Broekens, P., van Geel, B., Charman, D.J., Pancost, R.D., Chambers, F.M. and Evershed, R.P. (2008) The disappearance of Sphagnum imbricatum from Butterburn Flow, UK. *Holocene* **18**, 991-1002.

Naafs, B.D.A., Inglis, G.N., Zheng, Y., Amesbury, M.J., Biester, H., Bindler, R., Blewett, J., Burrows, M.A., del Castillo Torres, D., Chambers, F.M., Cohen, A.D., Evershed, R.P., Feakins, S.J., Gałka, M., Gallego-Sala, A., Gandois, L., Gray, D.M., Hatcher, P.G., Honorio Coronado, E.N., Hughes, P.D.M., Huguet, A., Könönen, M., Laggoun-Défarge, F., Lähteenoja, O., Lamentowicz, M., Marchant, R., McClymont, E., Pontevedra-Pombal, X., Ponton, C., Pourmand, A., Rizzuti, A.M., Rochefort, L., Schellekens, J., De Vleeschouwer, F. and Pancost, R.D. (2017) Introducing global peat-specific temperature and pH calibrations based on brGDGT bacterial lipids. *Geochim. Cosmochim. Acta* **208**, 285-301.

Nichols, J.E. and Huang, Y. (2007) C23–C31 n-alkan-2-ones are biomarkers for the genus Sphagnum in freshwater peatlands. *Org. Geochem.* **38**, 1972-1976.

728 Nott, C.J., Xie, S., Avsejs, L.A., Maddy, D., Chambers, F.M. and Evershed, R.P. (2000) n-
729 Alkane distributions in ombrotrophic mires as indicators of vegetation change related
730 to climatic variation. *Org. Geochem.* **31**, 231-235.
731 Pancost, R., Pressley, S., Coleman, J., Talbot, H., Kelly, S., Farrimond, P., Schouten, S.,
732 Benning, L. and Mountain, B. (2006) Composition and implications of diverse lipids in
733 New Zealand geothermal sinters. *Geobiology* **4**, 71-92.
734 Pancost, R.D., Baas, M., van Geel, B. and Sinninghe Damsté, J.S. (2003) Response of an
735 ombrotrophic bog to a regional climate event revealed by macrofossil, molecular and
736 carbon isotopic data. *Holocene* **13**, 921-932.
737 Pancost, R.D., Steart, D.S., Handley, L., Collinson, M.E., Hooker, J.J., Scott, A.C.,
738 Grassineau, N.V. and Glasspool, I.J. (2007) Increased terrestrial methane cycling at
739 the Palaeocene–Eocene thermal maximum. *Nature* **449**, 332-335.
740 Pearson, A., Flood Page, S.R., Jorgenson, T.L., Fischer, W.W. and Higgins, M.B. (2007) Novel
741 hopanoid cyclases from the environment. *Environ. Microbiol.* **9**, 2175-2188.
742 Peiseler, B. and Rohmer, M. (1991) Prokaryotic triterpenoids. (22R,32R)-34,35-
743 Dinorbacteriohopane-32,33-diols from Acetobacter aceti ssp. xylinum: new
744 bacteriohopane derivatives with shortened side-chain. *J. Chem. Soc.* 2449-2453.
745 Peters, K. and Moldowan, J. (1991) Effects of source, thermal maturity, and biodegradation
746 on the distribution and isomerization of homohopanes in petroleum. *Org. Geochem.*
747 **17**, 47-61.
748 Quirk, M., Wardroper, A., Wheatley, R. and Maxwell, J. (1984) Extended hopanoids in peat
749 environments. *Chem. Geol.* **42**, 25-43.
750 Ries-Kautt, M. and Albrecht, P. (1989) Hopane-derived triterpenoids in soils. *Chemical*
751 *Geology* **76**, 143-151.
752 Rohmer, M., Bouvier-Nave, P. and Ourisson, G. (1984) Distribution of hopanoid triterpenes in
753 prokaryotes. *Microbiol.* **130**, 1137-1150.
754 Rosa-Putra, S., Nalin, R., Domenach, A.-M. and Rohmer, M. (2001) Novel hopanoids from
755 Frankia spp. and related soil bacteria. *Eur. J. Biochem.* **268**, 4300-4306.

Sáenz, J.P., Grosser, D., Bradley, A.S., Lagny, T.J., Lavrynenko, O., Broda, M. and Simons, K. (2015) Hopanoids as functional analogues of cholesterol in bacterial membranes. *PNAS.* **112**, 11971-11976.

Schefuß, E., Eglinton, T.I., Spencer-Jones, C.L., Rullkötter, J., De Pol-Holz, R., Talbot, H.M., Grootes, P.M. and Schneider, R.R. (2016) Hydrologic control of carbon cycling and aged carbon discharge in the Congo River basin. *Nat. Geosci*.

Seifert, W.K. and Moldowan, J.M. (1980) The effect of thermal stress on source-rock quality as measured by hopane stereochemistry. *Phys. Chem. Earth* **12**, 229-237.

Serkebaeva, Y.M., Kim, Y., Liesack, W. and Dedysh, S.N. (2013) Pyrosequencing-based assessment of the bacteria diversity in surface and subsurface peat layers of a norther wetland, with focus on poorly studies phyla and candidate divisions. *PloS ONE*. **8**. p.e63994

Sessions, A.L., Zhang, L., Welander, P.V., Doughty, D., Summons, R.E. and Newman, D.K. (2013) Identification and quantification of polyfunctionalized hopanoids by high temperature gas chromatography–mass spectrometry. *Org. Geochem.* **56**, 120-130.

Sinninghe Damsté, J.S., Rijpstra, W.I.C., Schouten, S., Fuerst, J.A., Jetten, M.S. and Strous, M. (2004) The occurrence of hopanoids in planctomycetes: implications for the sedimentary biomarker record. *Org. Geochem.* **35**, 561-566.

Smittenberg, R., Pancost, R., Hopmans, E., Paetzel, M. and Damsté, J.S. (2004) A 400-year record of environmental change in an euxinic fjord as revealed by the sedimentary biomarker record. *Palaeogeogr, Palaeoclimatol. Palaeoecol.* **202**, 331-351.

Spencer-Jones, C.L., Wagner, T., and Talbot, H.M (2017) A record of aerobic methane oxidation in tropical Africa over the past 2.5 Ma. *Geochim. Cosmochim. Acta*. **218**. 27-39

Talbot, H.M., Bischoff, J., Inglis,.G.N., Collinson, M.E. and Pancost, R.D. (2016a) Polyfunctionalised bio- and geohopanoids in the Eocene Cobham Lignite. *Org. Geochem.* **96**, 77-92.

783 Talbot, H.M. and Farrimond, P. (2007) Bacterial populations recorded in diverse sedimentary
784 biohopanoid distributions. *Org. Geochem.* **38**, 1212-1225.
785 Talbot, H.M., Handley, L., Spencer-Jones, C.L., Dinga, B.J., Schefuß, E., Mann, P.J., Poulsen,
786 J.R., Spencer, R.G., Wabakanghanzi, J.N. and Wagner, T. (2014) Variability in aerobic
787 methane oxidation over the past 1.2 Myrs recorded in microbial biomarker signatures
788 from Congo fan sediments. *Geochim. Cosmochim. Acta* **133**, 387-401.
789 Talbot, H.M., McClymont, E.L., Inglis, G.N., Evershed, R.P. and Pancost, R.D. (2016b) Origin
790 and preservation of bacteriohopanepolyol signatures in Sphagnum peat from
791 Bissendorfer Moor (Germany). *Org. Geochem.* **97**, 95-110.
792 Torres, L.C. and Pancost, R.D. (2016) Insoluble prokaryotic membrane lipids in a Sphagnum
793 peat: Implications for organic matter preservation. *Org. Geochem.* **93**, 77-91.
794 Uemura, H. and Ishiwatari, R. (1995) Identification of unusual 17β (H)-moret-22 (29)-ene in
795 lake sediments. *Org. Geochem.* **23**, 675-680.
796 Van Dorsselaer, A., Ensminger, A., Spyckerelle, C., Dastillung, M., Sieskind, O., Arpino, P.,
797 Albrecht, P., Ourisson, G., Brooks, P. and Gaskell, S. (1974) Degraded and extended
798 hopane derivatives (C 27 to C 35) as ubiquitous geochemical markers. *Tetrahedron*
799 *Lett.* **15**, 1349-1352.
800 van Winden, J.F., Talbot, H.M., De Vleeschouwer, F., Reichart, G.-J. and Sinninghe Damsté,
801 J.S. (2012) Variation in methanotroph-related proxies in peat deposits from Misten
802 Bog, Hautes-Fagnes, Belgium. *Org. Geochem.* **53**, 73-79.
803 Zhang, Z., Wang, C., Qiu, X., Huang, X. and Xie, S. (2009) Occurrence of highly abundant
804 bacterial hopanoids in Dajiuhu peatland, central China. *Front. Earth. Sci. China* **3**, 320-
805 326.
806 Zheng, Y., Singarayer, J.S., Cheng, P., Yu, X., Liu, Z., Valdes, P,J. and Pancost, R.D (2014)
807 Holocene variations in peatland methane cycling associated with the Asian summer
808 monsoon system. *Nat. Comms*. **5**. 4631
809 Zheng, Y., Li, Q.Y., Wang, Z.Z., Naafs, B.D.A., Yu, X.F. and Pancost, R.D (2015) Peatland
810 GDGT records of Holocene climatic and biogeochemical responses to the Asian
811 Monsoon. *Org. Geochem*. **87**. 86-95

812 Zhong, Q., Chen, H., Liu, L., He, Y., Zhu, D., Jiang, L., Zhan, W and Hu, J (2017) Water table
813 drawdown shapes the depth-dependant variations in prokaryotic diversity and
814 structure in Zoige peatlands. *FEMS Micro. Eco.* **93**. fix049
815 Zundel, M. and Rohmer, M. (1985) Prokaryotic triterpenoids. *FEBS* **150**, 23-27.

816

Figure 1

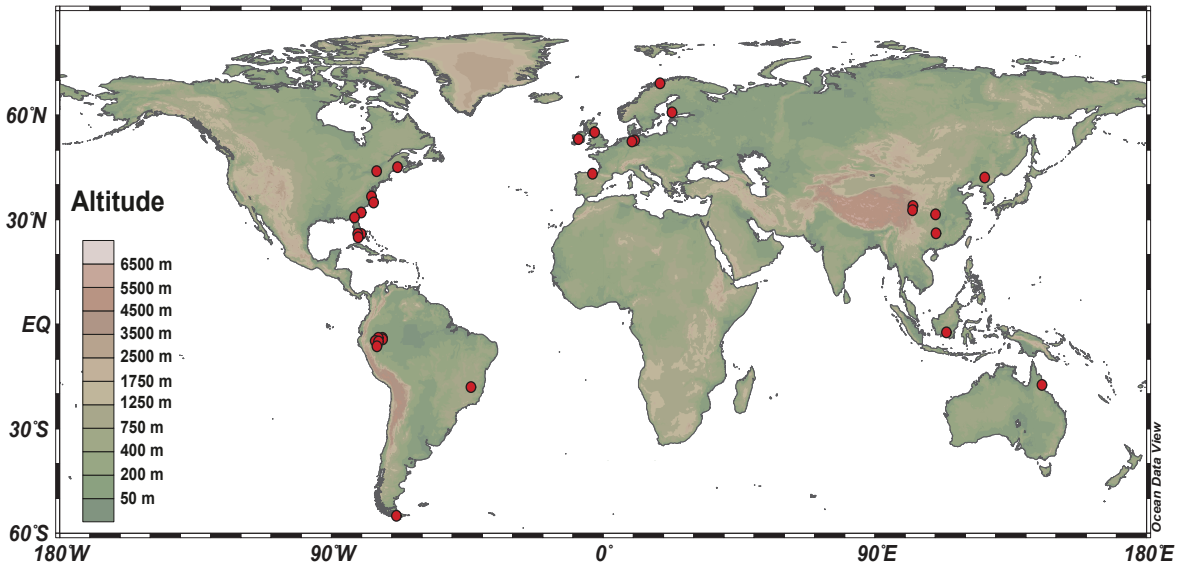
Altitude
6500 m
5500 m
4500 m
3500 m
2500 m
1750 m
1250 m
750 m
400 m
200 m
50 m
60˚N
30˚N
EQ
30˚S
60˚S
180˚W
90˚W
0˚
90˚E
180˚E
Ocean Data View

Figure 2

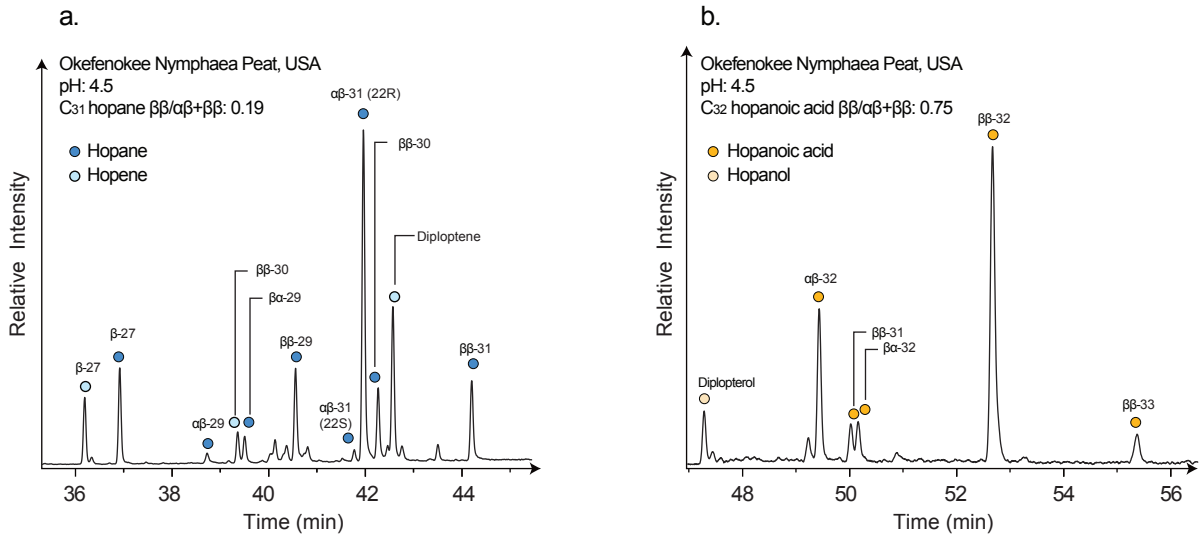
a.
Okefenokee Nymphaea Peat, USA
pH: 4.5
C31 hopane ββ/αβ+ββ: 0.19
Hopane
Hopene
Relative Intensity
β-27
β-27
αβ-29
ββ-30
βα-29
ββ-29
αβ-31 (22R)
αβ-31 (22S)
ββ-30
Diploptene
ββ-31
36
38
40
42
44
Time (min)
b.
Okefenokee Nymphaea Peat, USA
pH: 4.5
C32 hopanoic acid ββ/αβ+ββ: 0.75
Hopanoic acid
Hopanol
Relative Intensity
Diplopterol
αβ-32
ββ-31
βα-32
ββ-32
ββ-33
48
50
52
54
56
Time (min)

Figure 3

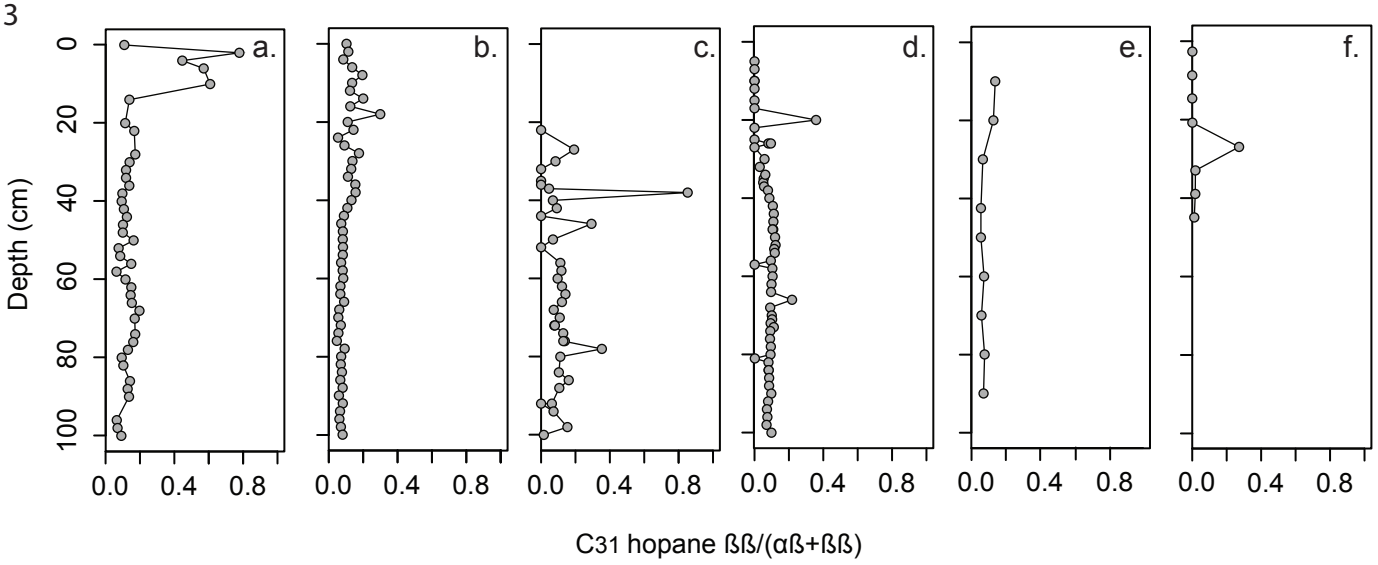

Figure 4

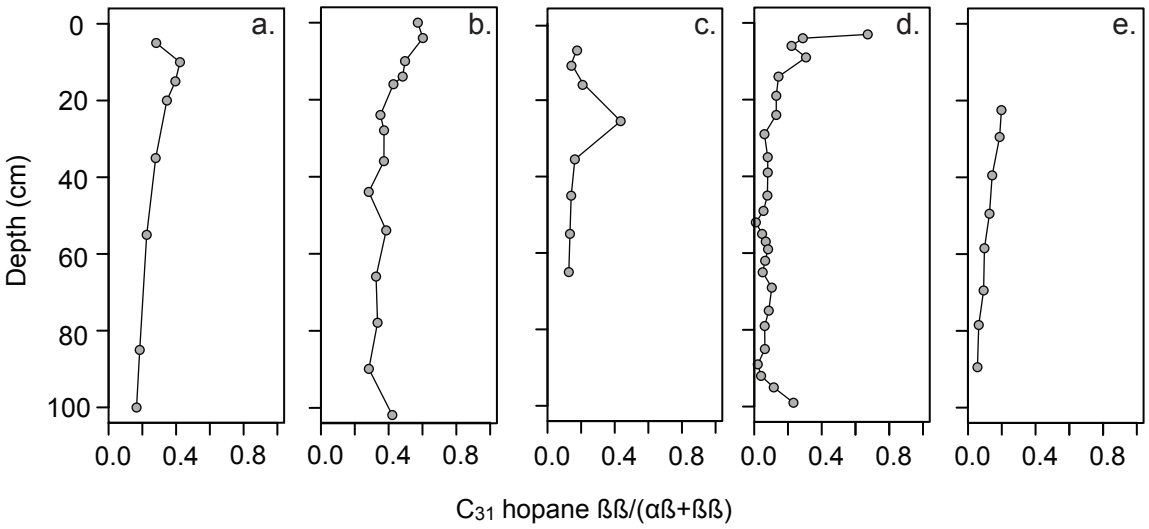

Figure 5

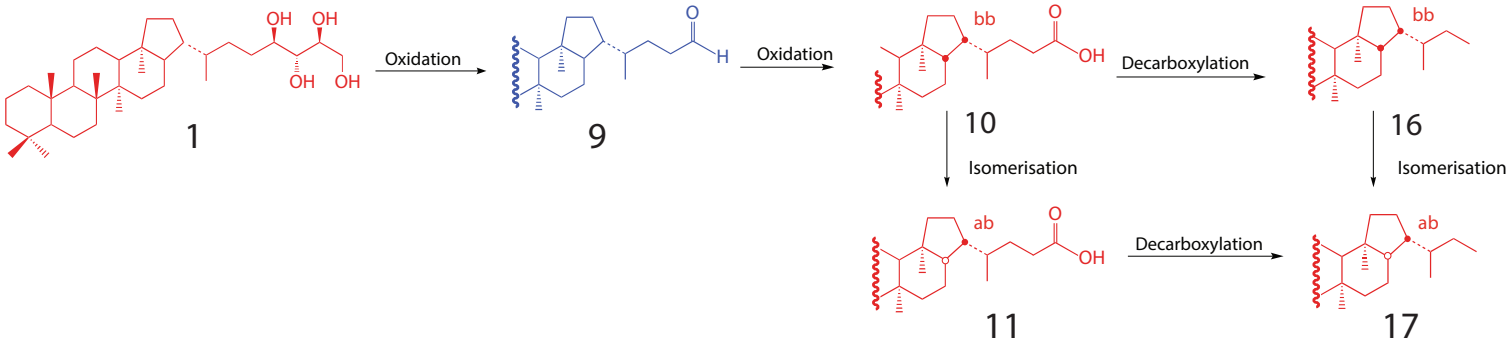
OH
OH
OH
OH
1
Oxidation
O
H
9
Oxidation
bb
O
OH
10
Decarboxylation
bb
16
Isomerisation
Isomerisation
ab
O
OH
11
Decarboxylation
ab
17

Figure 6

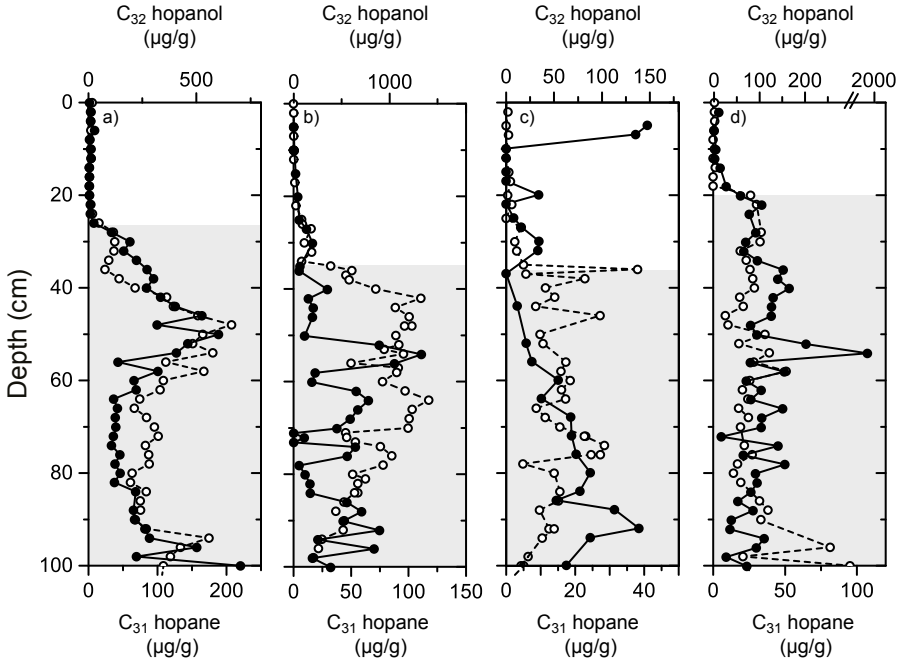
C32 hopanol (µg/g)
C31 hopane (µg/g)
Depth (cm)
a)
b)
c)
d)
0
500
1000
50
100
150
2000
20
40
60
80
200

Figure 7

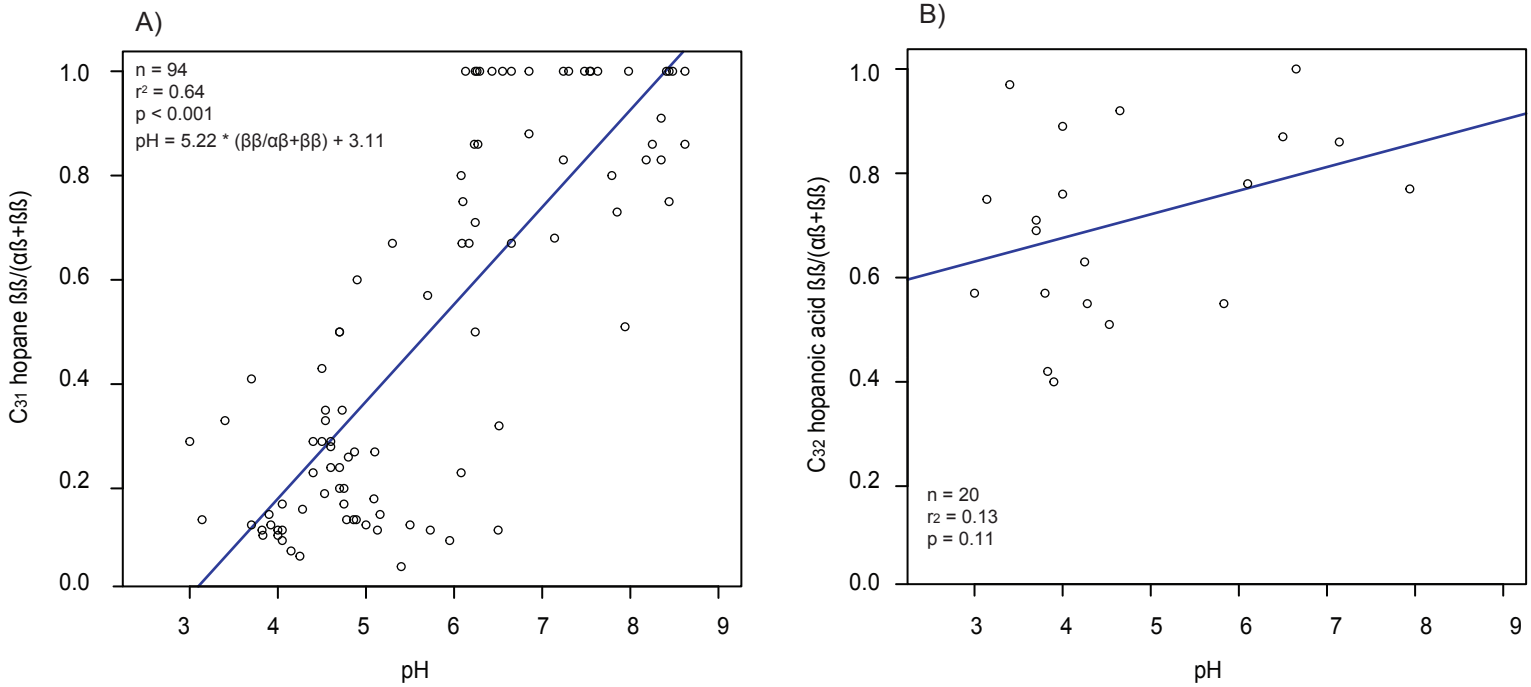
A)
n = 94
r² = 0.64
p < 0.001
pH = 5.22 * (ββ/αβ+ββ) + 3.11
C31 hopane ββ/(αβ+ββ)
pH
B)
n = 20
r2 = 0.13
p = 0.11
C32 hopanoic acid ββ/(αβ+ββ)
pH

Figure 8

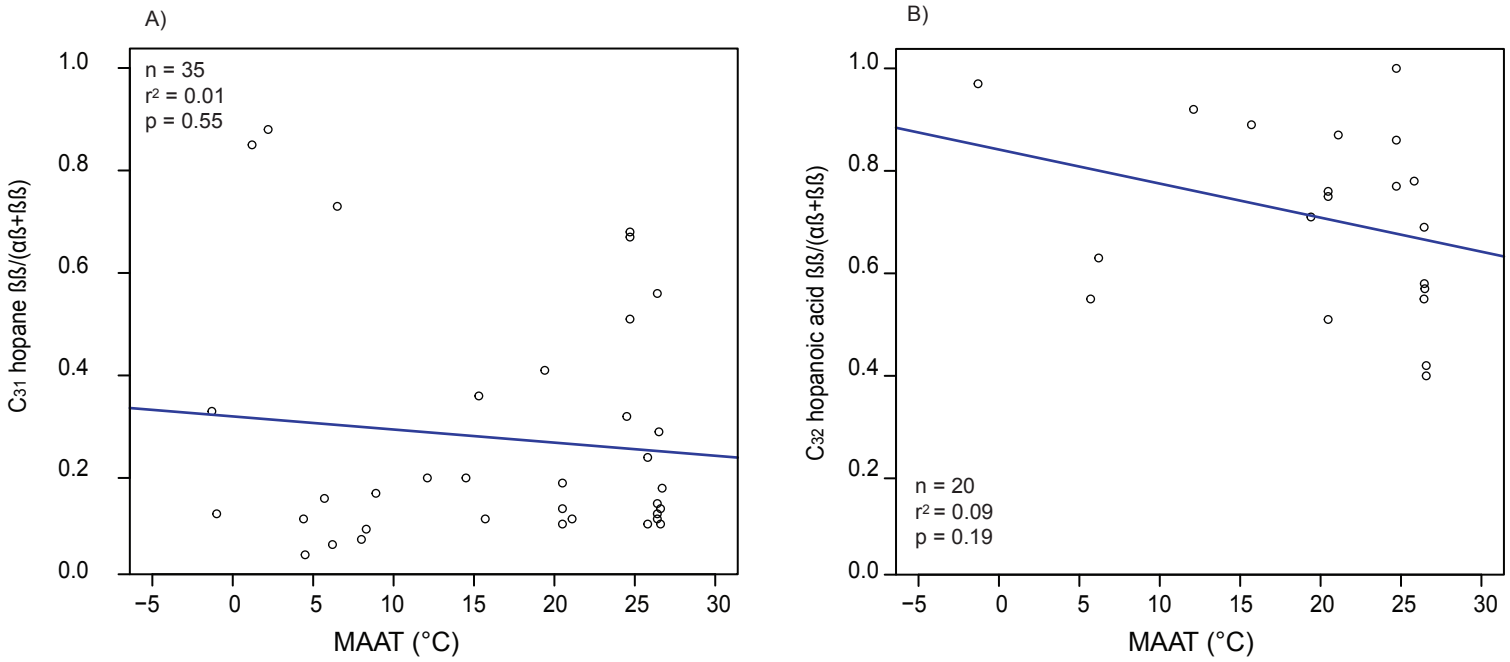
A)
n = 35
r² = 0.01
p = 0.55
C31 hopane ßß/(aß+ßß)
MAAT (°C)
B)
n = 20
r² = 0.09
p = 0.19
C32 hopanoic acid ßß/(aß+ßß)
MAAT (°C)

Figure 9

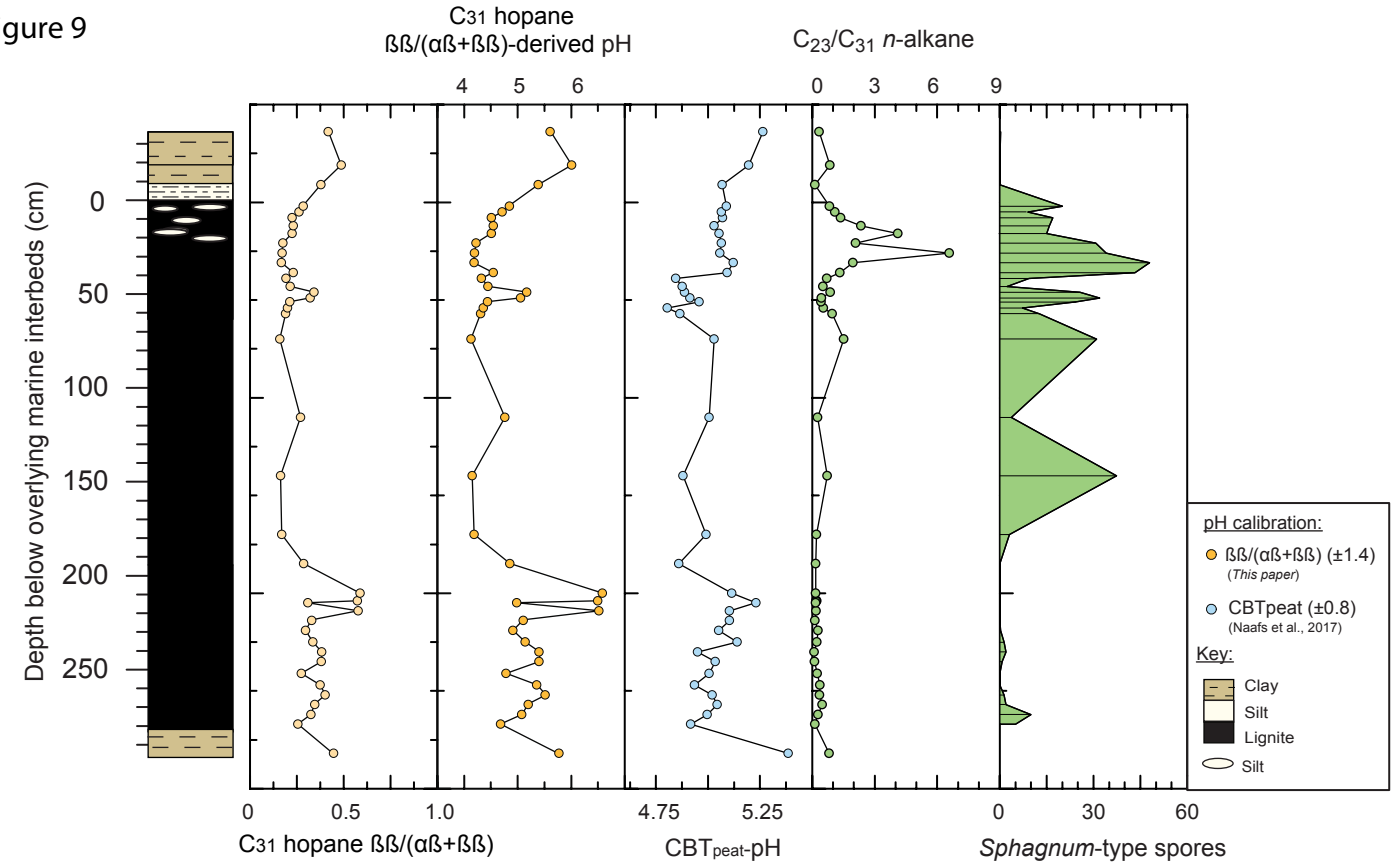
C31 hopane
ßß/(αß+ßß)-derived pH
C23/C31 n-alkane
4
5
6
0
3
6
9
Depth below overlying marine interbeds (cm)
0
50
100
150
200
250
0
0.5
1.0
C31 hopane ßß/(αß+ßß)
4.75
5.25
CBTpeat-pH
0
30
60
Sphagnum-type spores
pH calibration:
ßß/(αß+ßß) (±1.4)
(This paper)
CBTpeat (±0.8)
(Naafs et al., 2017)
Key:
Clay
Silt
Lignite
Silt